# FULLERENE TRANSPORT IN SATURATED POROUS MEDIA


*Xin (Cissy) Ma[1], Sheldon Skaggs[2], Dermont Bouchard[1]*, James Weaver[1], Carl Isaacson[3],*

*USEPA Office of Research and Development, National Exposure Research Laboratory[1]*
*Student Services Contractor[2], National Research Council Research Associate[3], Athens, GA, USA*
*Corresponding author* phone: (706) 355-8333; email: bouchard.dermont@epa.gov*


## Introduction

- Exposure to fullerenes ($C_{60}$ and its derivatives) have resulted in potential human and aquatic toxicities as well as antibacterial effects.
- Understanding of the fullerenes fate and transport mechanisms is limited.
- Previous studies shown that when $C_{60}$ is mixed in water it forms kinetically stable colloidal suspensions (*aqu*/$C_{60}$).
- Although the formation of *aqu*/$C_{60}$ is pH and ionic strength dependent, the suspensions are highly negatively charged under varying solution conditions.
- The mobility of these highly charged colloidal aggregates is unknown.
- It is also unknown whether existing particle transport models adequately describe *aqu*/$C_{60}$ transport in water-saturated porous media.

## Methods and Materials

- The 125 µm to 250 µm size fraction of Iota sand was DDI-washed and wet-packed in an Omnifit column (100 mm x 25 mm ID).
- *Aqu*/$C_{60}$ suspensions were continuously stirred in various buffers for > 111 days. The buffers were either acetate (pH = 4.00 ± 0.01), HEPES (pH = 7.01 ± 0.04), or Tris (pH = 10.03 ± 0.06). Ionic strength was equivalent to 10 mM NaCl.
- The hydrodynamic diameters and zeta ($\zeta$) potentials of the *aqu*/$C_{60}$ suspensions were analyzed by dynamic light scattering.
- The pH titrations were performed using an autotitrator in conjunction with real time monitoring of size and $\zeta$-potential changes.
- The streaming potentials of Iota sand in various buffers were measured using a SurPass electrokinetic analyzer.

## Model

- Mathematical Model: 2nd order non-linear sorption on covered and noncovered sites.

$$\frac{\partial C}{\partial t} = D_h \frac{\partial^2 C}{\partial x^2} - v\frac{\partial C}{\partial x} - \frac{\rho_b}{\theta_w}\frac{dS}{dt}$$

$$\frac{dS}{dt} = \frac{\theta_w}{\rho_b}\left(k_{att-nc}\, f_{nc} + k_{att-c}\, f_c\right)C - k_{det} S$$

C = aqueous concentration
S = sorbed concentration
$D_h$ = dispersion coefficient
v = interstitial fluid velocity
$\rho_b$ = bulk density
$\theta_w$ = water-filled porosity
$S_{max}$ = max. sorbed conc.
$k_{att}$ = attachment coefficient (noncovered or covered) sites
$k_{det}$ = detachment coefficient

$$f_{nc} = \frac{S_{max} - S}{S_{max}}$$

$$f_c = \frac{S}{S_{max}}$$

$$k_{att} = \frac{3}{2}\left(\frac{1-\theta_w}{d_c}\right) v\,\alpha\,\eta_o$$

$d_c$ = avg soil grain diameter
$\alpha$ = attachment (collision) efficiency
$\eta_o$ = single-collector contact efficiency

- Solutions strategies – Method of Lines
  - ❖ Discretize space using Eulerian-Lagrangian Operator Splitting

$$\frac{dx}{dt} = v$$

$$\frac{DC}{Dt} = D_h \frac{\partial^2 C}{\partial x^2} - \frac{\rho_b}{\theta_w}\frac{dS}{dt}$$

❖Eliminates numerical disperson of 1st order methods

❖Eliminates oscillation of classical 2nd order methods

- ❖ Solve time via ordinary differential equation solver

## Results

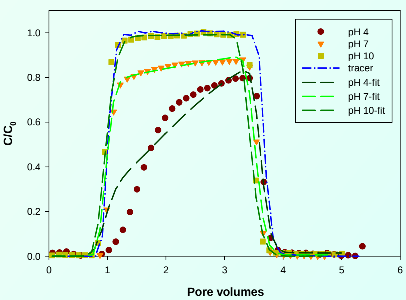


**Figure 1. Measured and simulated *aqu*/$C_{60}$ breakthrough curves under different pH in saturated quartz sand columns**

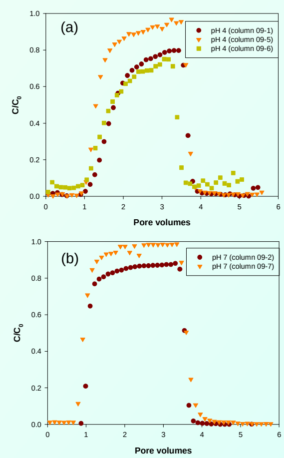


| Column | $\alpha$ | $K_{att}$ (1/hr) | $S_{max}$ | $C_0$ (mg/L) |
|---|---|---|---|---|
| 09-1 | 0.150 | 5.14 | 0.15 | 0.41 |
| 09-5 | 0.090 | 3.14 | 0.05 | 0.35 |
| 09-6 | 0.205 | 7.57 | 0.40 | 0.17 |
| average | 0.148 | 5.29 | 0.20 | 0.31 |

| Column | $\alpha$ | $K_{att}$ (1/hr) | $S_{max}$ | $C_0$ (mg/L) |
|---|---|---|---|---|
| 09-2 | 0.030 | 1.05 | 0.25 | 1.30 |
| 09-7 | 0.015 | 0.45 | 0.05 | 1.35 |
| average | 0.023 | 0.75 | 0.15 | 1.33 |

**Figure 2. Replicate breakthrough curves of *aqu*/$C_{60}$ in pH 4 (a) and pH 7 (b).**

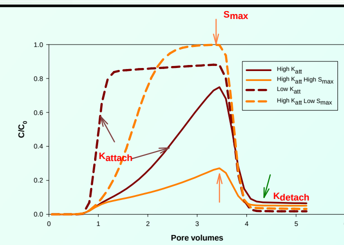


**Figure 3. Simulated breakthrough curves show the effects of $K_{att}$ and $S_{max}$.**

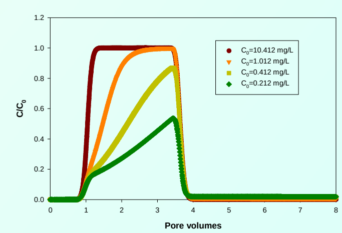


**Figure 4. The effect of initial concentration ($C_0$) on the simulated breakthrough curves.**

## Results

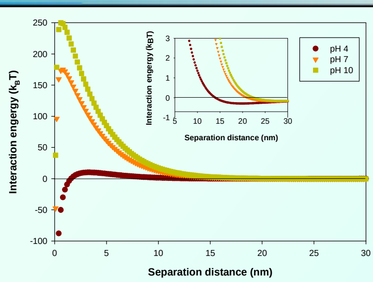


**Figure 5. DLVO interaction energy profiles as a function of pH for *aqu*/$C_{60}$. The secondary minimums under different pH shown in the insert.**

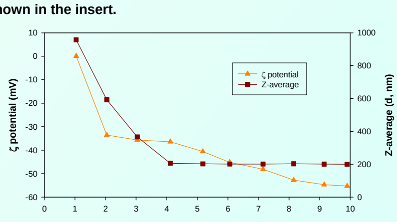


**Figure 6. $\zeta$ potential and Z-average diameter of unfiltered *aqu*/$C_{60}$ in pH 10 titrated as a function of pH.**

- The *aqu*/$C_{60}$ at high pH showed more mobility through porous media than at low pH (Figure 1).
- For *aqu*/$C_{60}$ generated under different pH, the attachment efficiencies ($\alpha$) are significantly different (Figure 2).
- The *aqu*$C_{60}$ suspensions formed were pH sensitive (Figure 5 and 6).
- The aggregates in aqueous systems were highly negatively charged (Figure 6).
- The frontal region of the curves is controled by $\alpha$ while maximum sorbed concentration ($S_{max}$) controls the height of the curves (Figure 3).
- Initial concentrations of *aqu*/$C_{60}$ greatly influence the shapes of breakthrough curves (Figure 4).
- Both linear and non-linear models can describe the breakthrough curves of *aqu*/$C_{60}$ at pH 10.
- Details of the breakthrough curves of *aqu*/$C_{60}$ in pH 4 are not well modeled by the nonlinear model, even when covered sites are included.

## Conclusions

- The solution chemistry affects the transport in porous media.
- The *aqu*/$C_{60}$ aggregates have high negatively charged surfaces.
- *Aqu*/$C_{60}$ is highly mobile as pH increases.
- The existing non-linear model with no covered area included may not accurately describe the *aqu*/$C_{60}$ transport under acidic condition (highly sorbed).


## Acknowledgement

The authors thank Bethany Wigington, Tantiana Burns and Sung Gon Lee for the assistance of sample analysis.